MARY KAY O'CONNOR PROCESS SAFETY CENTER
TEXAS A&M ENGINEERING EXPERIMENT STATION

20th Annual International Symposium
October 24-26, 2017 • College Station, Texas

Dynamic Response of Vertical Tank Impacted by Blast Fragments in Chemical Industrial Parks

Guohua Chen†, Shuai Qi, Kun Hu, Chilou Zhou*

Institute of Safety Science and Engineering, South China University of Technology, Guangzhou 510640, China

† Presenter E-mail: mmghchen@scut.edu.cn

* Corresponding author: mezcl@scut.edu.cn

Abstract

The adjacent vessels may be impacted and/or destroyed by blast fragments in chemical industrial parks or plants, which could lead to the domino effects. Based on the analysis of common parameters of blast fragments including the shape, quantity, mass, and impact velocity, the numerical model of vertical storage tanks impacted by blast fragments was developed with LS-DYNA. Considering deformation of the fragment itself, the law of the dynamic response of vertical tank was described quantitatively. The results showed that there were 3 collisions during the impact process, the maximum plastic deformation occurred at the impact center, the plastic strain was mainly distributed in the range from the impact center to the tank bottom, and there were 4 plastic hinge lines in the deformation region. There was linear relationship between the residual displacement of impact center and the impact velocity of the fragment, and the tank wall had entered plastic deformation stage. With the horizontal impact angle in the range from 15° to 30°, the plastic deformation energy of the tank increased with the horizontal impact angle evidently; with the horizontal impact angle in the range from 30° to 35°, the impact mode of the fragment was changed from penetrating the tank wall to sliding along the tank wall; with the horizontal impact angle in the range from 35° to 60°, the deformation energy of the tank decreased linearly with horizontal impact angle, and the influence of vertical impact angle on the deformation energy of the tank was greatly reduced.

Introduction

Impact load has the characteristics of unidirectional action, short duration and large shock

amplitude, once acts on a tank in chemical industrial parks or plants, it could cause medium leakage, fire, explosion and other accidents. European standard EN 14620-1 clearly stipulates that the impact of flying objects on the tank should be considered when the LNG tanks are designed, and the flying object with mass of 50kg and velocity of 45m/s is recommended for impact calculation (EN 14620-1, 2006). Arros et al. [1] developed a simulation model of Boeing 747 using LS-DYNA, and the hit against the shell structure was studied. Atkinson et al. [2] investigated the consequences of LNG tanks subjected to conventional weapon attacking by numerical simulation, which showed that the tank would vibrate violently and led to destruction of the outer tank, continuous attacking would cause liquid leakage and fire. Wang et al. [3] analyzed the response of water tank under explosion load with LS-DYNA, and the influence of filled medium and boundary on anti-explosion performance of the tank was studied quantitatively. Cui et al. [4] performed a study on the mechanical performance of LNG tank under the impact of BGM-109 cruise missile by LS-DYNA, and it was found that the maximum stress zone of the tank was greatly affected by the initial velocity of missile.

In addition to aircraft, missile impact and explosive load, the fragment generated from chemical vessels is also an important source of impact load, which can be projected over long distances, lead to damage of other nearby equipment, and may cause domino effect [5, 6]. Mébarki et al. [7] proposed a method for calculating the three-dimensional trajectory of fragments generated from a horizontal tanks , which considered the aerodynamic drag of projection. It was found that the failure of target tanks would occur once the impact depth reached the tank wall thickness, or the residual wall thickness was smaller than the critical value. And the failure probability model of the target tank was established [8]. Based on the assessment method of loss area of a vessel shell, Chen et al. [9] proposed a failure criterion of the tank under the impact of fragments by considering the critical residual strength factor. Until now, the research on the domino effects caused by blast fragments mainly focuses on the probability assessment of projection, impacting and destroying target tanks, reports on the quantitative description of the damage effects of fragments impacting on the tank are scare. Pan et al. [10] analyzed the dynamic response of the vertical tank impacted by the cylinder and cuboid fragments by using LS-DYNA, the results showed that cuboid fragments impacting on the tank caused more serious effect on the tank structure strength, the maximum loss intensity of the tank occurred when impact angle was 10°. The 1/10 spherical tank impacted by cuboid fragment was simulated by Luo et al. [11], the whole failure stages were divided into invasion, erosion, perforation and penetration. Most of the existing researches took fragments as ideal geometry, ignoring their geometrical irregularities in chemical accidents, and the selection of fragment parameters, such as mass and impact velocity, is lack of reason. In addition, as the fragment is taken as rigid, the deformation of the fragment itself cannot be considered during the impact process.

In this paper, a finite element model of large vertical tanks subjected to the impact of the

fragment was developed using LS-DYNA, a reasonable constitutive model was adopted in consideration of the elastic-plastic deformation of the fragment during the impact process, and the dynamic response of large vertical tanks under the impact of a fragment was described quantitatively. The shape, quantity, mass, velocity and other parameters of fragments were analyzed in detail. The results will be useful for the design, improvement and safety protection of storage tanks.

Finite element modelling

Structure of large vertical tanks

The dome roof tank belongs to vertical tanks, and its basic structure includes tank roof, tank wall, tank bottom, and accessories. It is widely used because of its simple structure and convenient construction. According to Chinese standard "Code for construction of vertical cylindrical steel welded storage tanks" [12], the vertical tanks with the volume of 2000m^3, 5000m^3, 10000m^3 and 20000m^3 are selected as the targets impacted by fragments. The dimension parameters of the above tanks are shown in Table 1, and the sizes of each shell plate of the tank wall are shown in Table 2.

Table 1 Dimension parameters of large dome roof tanks

Parameters	TK1	TK2	TK3	TK4
Volume (m^3)	2000	5000	10000	20000
Diameter (m)	15.78	23.70	31.00	42.00
Height of Tank wall (m)	11.37	12.53	14.58	17.00
Height of Dome roof (m)	1.721	2.573	3.368	4.546

Table 2 Sizes of each shell plate (height ×thickness)

Num. of shell plate	TK1(mm)	TK2(mm)	TK3(mm)	TK4(mm)
1	1895×11	1790×14	1620×20	1700×23
2	1895×9	1790×12	1620×18	1700×21
3	1895×8	1790×10	1620×16	1700×19
4	1895×7	1790×9	1620×14	1700×17
5	1895×6	1790×7	1620×12	1700×14
6	1895×6	1790×6	1620×10	1700×11
7	--	1790×6	1620×8	1700×9
8	--	--	1620×7	1700×9
9	--	--	1620×7	1700×9

10	--	--	--	1700×9

Since the wall thickness of a large vertical tank is much smaller than the diameter and height of the tank, the vertical tank is meshed with shell elements, and fixed constraints are applied to the tank bottom. The storage medium is crude oil with the density of 810 kg/m^3, and the filling ratio is 0.8. Generally, the crude oil in the tank remains stationary, the impact of the fragment on the tank wall is transitory, therefore, the crude oil is assumed as static, and the hydrostatic pressure is applied to the inner surface of the tank based on the height distribution. For instance, for TK3, the hydrostatic pressure in the bottom of the tank is 92.59 kPa, while that at the height of 11.664 m is 0 kPa. The geometric model of the tank is shown in Fig.1.

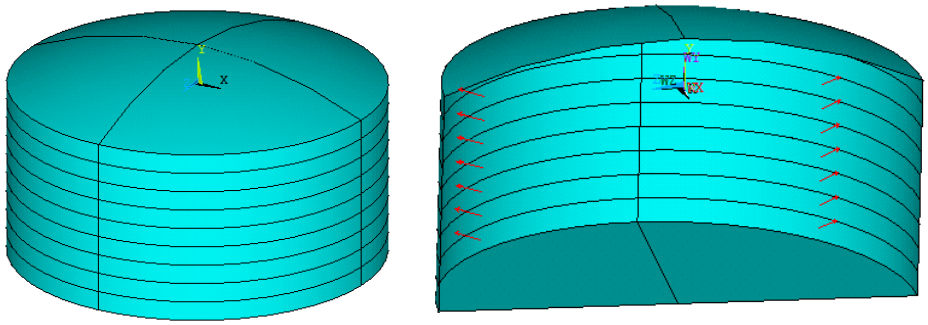

Fig.1 Geometric model of TK3

Parameters of blast fragments

Gubinelli et al. [13, 14] performed statistics on the explosion accidents of chemical vessels, the result showed that the maximum number of accidents occurred in horizontal tanks. Especially, the common shape of fragments exhibited as end cap-shaped and plate-shaped, as shown in Fig.2. According to Chinese code “Steel liquefied petroleum gas horizontal tank type and basic parameters” (NB/T 47001-2009) [15], a hemispherical head horizontal tank with 150m^3 is set as the chemical vessel in which the initial accident occurred. The material of the cylinder and head is 16MnR, with density of 7850 kg/m^3, and design pressure of 1.77 MPa, the parameters are shown in Table 3.

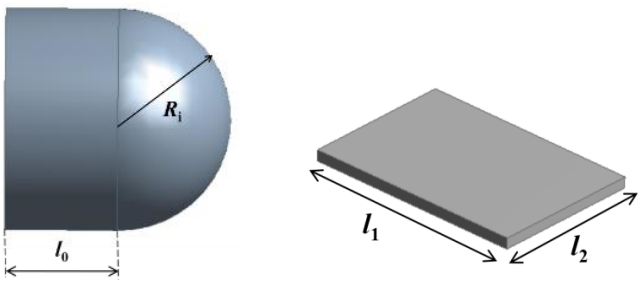

Fig.2 Schematic of common blast fragments

Table 3 Parameters of the horizontal tank

Volume (m^3)	Head type	Cylinder length (m)	Head height (m)	Wall thickness of Horizontal tank s(mm)
150	Hemispherical head	16.5	1.6	18

According to the calculation method of explosion energy of gas pressure vessels [16], kinetic energies of scaling factor distribution proposed by the Center for Chemical Process Safety[17], and the mass and velocity calculation method of fragments proposed respectively by Nguyen et al. [8] and Mébarki et al. [18], the parameters of fragments generated from the 150m^3 horizontal tank due to explosion are shown in Table 4.

Table 4 Parameters of 150 m^3 hemispherical head horizontal tank

Fragment type	Maximum projection energy E_{max}(kJ)	Minimum projection energy E_{min}(kJ)	Maximum mass $m_{max}^{end\text{-}cap}$(kg)	Minimum mass $m_{min}^{end\text{-}cap}$(kg)	Maximum velocity $v_{max}^{end\text{-}cap}$(m/s)	Minimum velocity $v_{min}^{end\text{-}cap}$(m/s)
End caps	1.06×10^4	4.09×10^3	25723	2297	96.1	17.8
Plates	1.06×10^4	4.09×10^3	23426	--	--	18.7

Material properties

The material of dome roof tanks is selected as 20R, its material properties are shown in Table 5. The material of fragments generated from the 150 m^3 hemispherical head horizontal tank is 16MnR, which is a kind of low alloy steels. The material parameters of fragments are shown in Table 6.

Table 5 The material parameters of dome roof tank

Density ρ_t(kg/m^3)	Elasticity Modulus E_t(MPa)	Poisson ratio μ	Shear modulus G_t(MPa)	Initial yield stress σ_0(MPa)	Fracture strain
7800	2.13×10^5	0.282	8.31×10^4	325	0.05

Table 6 The material parameters of fragments

Density ρ_t(kg/m^3)	Elasticity modulus E_t(MPa)	Poisson ratio μ	Shear modulus G_t(MPa)	Initial yieldσ_0(MPa)	Fracture strain

7850	2.09×10^5	0.28	8.20×10^4	345	0.05

Both the vertical tank and fragments are modeled with the elastic-plastic material model. In this material model, the Cowper-Symonds model is adopted to capture the strain rate effects and failure, as shown below:.

$$\sigma_Y = \sigma_0[1 + (\frac{\dot{\varepsilon}_{eff}^P}{C_S})^{1/P_S}] \quad (1)$$

Where σ_Y is the flow yield stress, σ_0 is the initial yield stress, $\dot{\varepsilon}_{eff}^P$ is the effective plastic strain rate, C_s and P_s are the strain rate parameters of Cowper-Symonds model. In this study, the strain rate parameters C_s and P_s are 40.4 and 5 both for 20R and 16MnR [19].

The contact behavior between the fragment and the vertical tank is defined as eroding contact, allowing high kinetic energy fragment to perforate the tank wall and penetrate along the remaining interior surface when the exterior surface experiences material failure during contact. The finite element model of the fragment and the vertical tank before contact is shown in Fig.3.

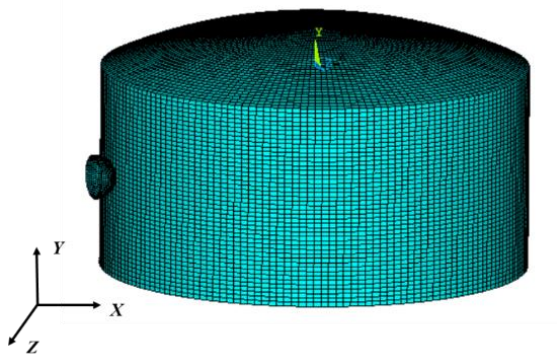

Fig.3 The finite element model of tank and fragment

Model Validation

A test system for modeling the impact process of fragments on the tank is shown in Fig.4. The semi cylindrical shell with diameter of 300 mm and height of 300 mm are used for modeling the small-scale vertical tank, and the conical projectiles with diameter of 7.82 mm in big end are adopted to model the small-scale fragment. The base of the small-scale vertical tank is fixed with different inclination angles to obtain various impact angles. Then the shots of projectiles with striking angles of 0°, 15°, 30°, 45° on the small-scale tank targets are carried out, and the striking velocity and residual velocity of the projectile are measured with two infrared velocimeters. The process of the projectile impact on the small-scale tank is also simulated using LS-DYNA,

and the residual velocity between the simulation and experimental result is compared in Table 7.

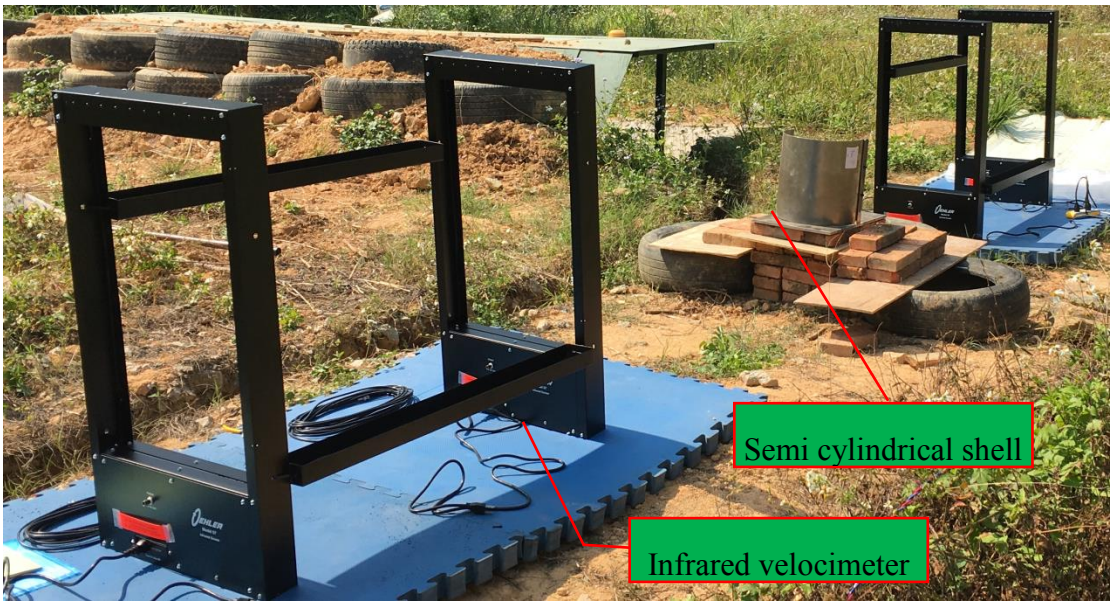

Fig. 4 The impact test set-up

Table 7 Comparison of residual velocity between the simulation and experiment result

Num.	Wall thickness of small-scale tanks h (mm)	impact angle θ (°)	Experiment results v_r (m/s)	Simulation results v_{sr} (m/s)	Error (%)
1	1.0	0	826	824	-0.24
2	1.5	0	828	833	0.60
3	2.0	0	813	828	1.85
4	2.75	0	765	771	0.78
5	1.0	15	842	841	-0.12
6	1.5	15	836	840	0.48
7	2.0	15	809	827	2.22
8	2.75	15	779	796	2.18
9	1.0	30	843	844	0.12
10	1.5	30	819	833	1.71
11	2.0	30	801	817	2.00
12	2.75	30	775	793	2.32
13	1.0	45	836	840	0.48
14	1.5	45	812	830	2.22
15	2.0	45	786	811	3.18
16	2.75	45	761	769	1.05

Through the comparison of the results, it is found that the maximum error is 3.18%, the minimum error is 0.12%, and the average error is 1.30%. The simulation results are slightly bigger than the experimental results except the cases in No.1 and No.5. It can be concluded that the simulation results show good agreements with experimental data, which indicates that the developed numerical model is reasonable, and it can be used to predict the dynamic response behavior of vertical tanks under impulsive loading.

Results and discussion

Impact process and deformation

The fragment, end cap-shaped, with mass of 2297 kg was taken to impact the vertical tank, TK3, at a speed of 60m/s, and the impact position occurs in the middle section of the tank wall. Fig.5 shows the time-history of the velocity in the midpoint of the impact region for the fragment and the tank. Fig.6 reveals the impact force-time curve of the tank.

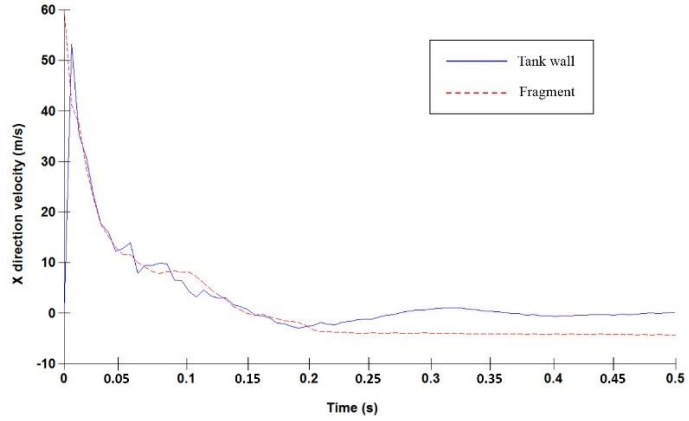

Fig. 5 The impact-point velocity history for the fragment and tank

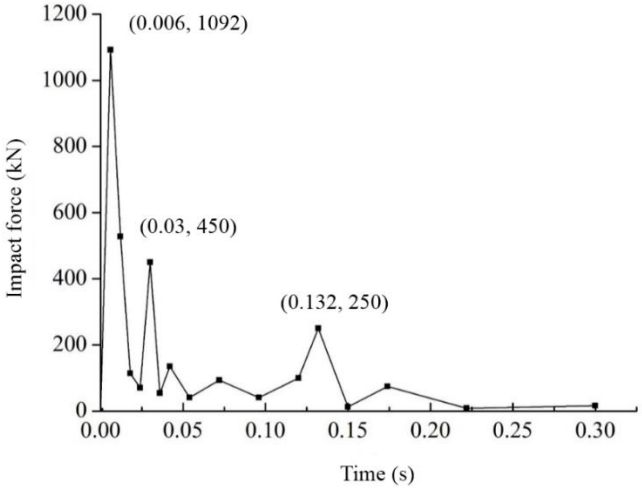

Fig.6 The impact force time history of the tank

As shown in Fig.6, the nonlinear characteristic of the time-history curve of impact force is obvious. It shows that the process of the fragment impact on the tank includes multiple collisions rather than only one collision. From the impact force-time curve of the tank, the impact force is in oscillatory condition from peak to trough and back to the peak, there are 3 main peaks, and the impact force-time curve oscillates in a small amplitude tending to be stable after 0.2 s. Once the high velocity fragment comes into contact with the tank, the velocity of the midpoint of the tank would instantly increase to the same value as the fragment. The first peak of the impact force, the highest one of 3 peaks, is 1092 kN at 0.006 s.

From Fig.5, the velocity of the impact point of the tank reaches its maximum value of 53.42 m/s at 0.007 s, then because of the restriction effect of the region near the impact point, the velocity of the tank reduces to the same value as the fragment, and the impact force is also decreased. The velocity of the tank is less than that of the fragment at 0.012 s, then the second peak of impact force forms at 0.03 s, which indicates the second collision occurs. The tank and the fragment have the same velocity at 0.09 s, because of the restriction effect of the tank top and the bottom plate, the hit-point velocity of the fragment is higher than that of the tank in the subsequent period, forming the third impact force peak at 0.132 s. Then the hit-point velocity of both the tank and the fragment decreases gradually to 0. After 0.156 s, the hit-points of both the tank and the fragment produce reverse velocity, indicating that the tank has enough resistance ability, the fragment is rebounded, and the elastic deformation of the tank will recover.

Fig.7 shows the plastic strain distribution of the tank after impact. The main deformation of the tank wall appears near the impact center, in the triangle region consisted of point A and B on the tank top and point C on the tank bottom. The whole triangular deformation region was sunken, the sunken degree of the triangle region ADE and BDF is larger than that of the triangle region DEF, therefore, there are 2 convex fold (DE and DF) on the tank wall, as well as the boundary between the deformation and non-deformation region (AC and BC), there is obvious plastic deformation near the 4 lines described above, which forms 4 plastic hinge lines.

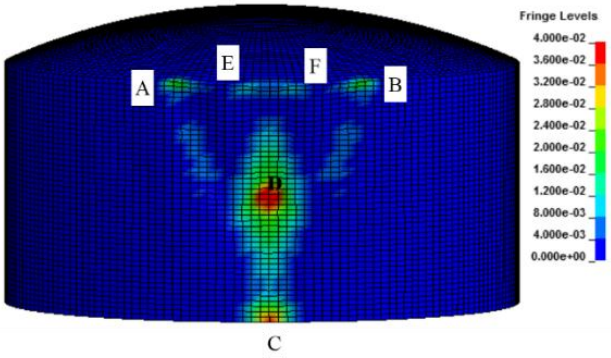

Fig.7 Plastic strain distribution of the tank

Effect of the tank volume

The fragment, end cap-shaped, with mass of 2297 kg, was used to impact the TK1, TK2, TK3 and TK4 at 60 m/s, TK1 is penetrated, while the fragments are all bounced for other cases. Fig.8 shows the impact force-time curve for TK2, TK3 and TK4. It is observed that each curve has 3 major peaks, which indicated that 3 major collisions occur during each impact process. The first collision time is independent of the tank volume, which is 0.006 s for all the cases. And the maximum impact force of the impact center is 1092 kN. The second collision time was almost the same, and the third collision time depends on the tank volume. The larger the tank volume is, the longer time spreading to tank top and bottom it takes. Therefore, the third collision time of TK4 was much longer than TK2 and TK3. The elastic deformation region of TK4 is wider, the restoring ability is stronger, and the restriction effect is more obvious, thus the impact force in third collision for TK4 is the biggest.

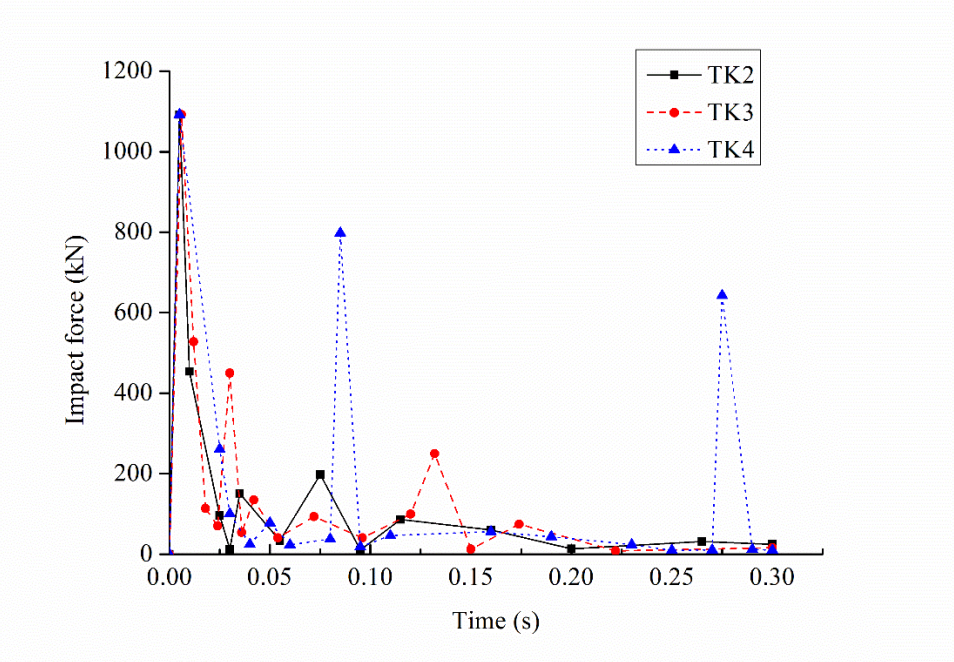

Fig.8 Impact force versus time curve

Effect of impact height

The fragment, end cap-shaped, with mass of 2297 kg, was used to impact the TK3 at 60 m/s with the hit height of 5 m, 7 m, 9 m and 12 m, respectively. Fig.9 shows the displacement of impact center-time curve. The tank wall thickness is 7 mm and there is not internal pressure when the

impact height is 12 m. The tank wall ruptured when the displacement of impact center reached 0.28 m, then the fragment penetrated the tank wall, most of the kinetic energy consumed on the penetration damage, therefore both the displacement of impact center and the deformation region of the tank wall were relatively small. The curve for impact height of 5 m, 7 m, and 9 m were roughly consistent, the tank wall was not broken, and the elastic deformation region recovered. There was still some residual deformation, which showed that the plastic deformation occurred. The tank wall thickness, stiffness and pressure were larger when the impact location was closer to the tank bottom, therefore, the deformation was more difficult, and the displacement of impact center-time curve for impact height of 5 m was in the lowest position, it indicated that the plastic deformation for impact height of 5 m was the minimum. The deformation of the tank wall was the maximum when impact height was 9 m. Overall, the higher the impact location is, the more sensitive to damage the tank becomes.

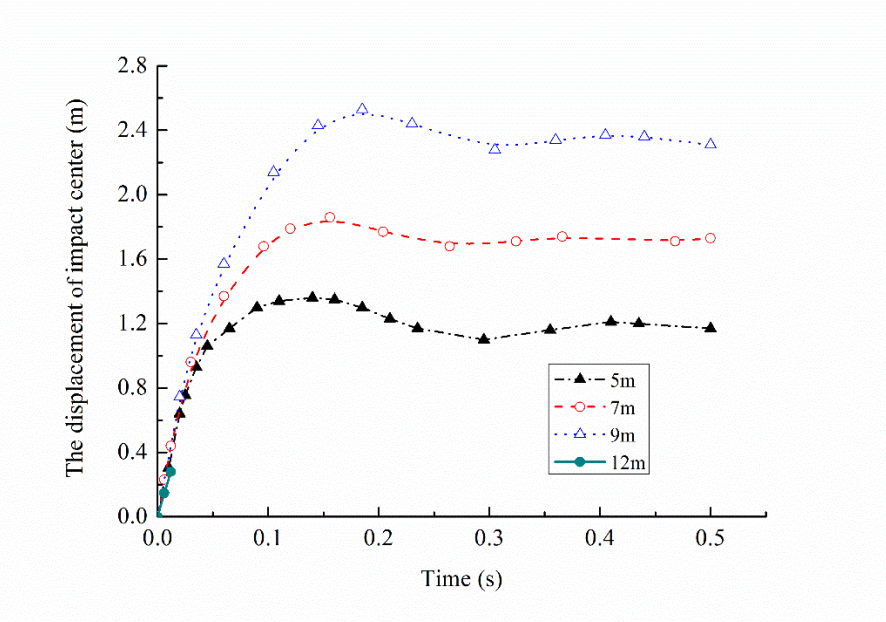

Fig.9 The displacement of impact center-time curve

Effect of fragment type

Two types of fragment, namely, end cap-shaped with mass of 2297 kg, and plate-shaped with size of 4 m×4 m and mass of 2260.8 kg, are used to simulate the impact on the TK3 at 60 m/s, respectively. The different impact postures of fragments would cause different contact area, which leads to different response. Two impact postures for each fragment are analyzed, and a total of 4 impact postures are shown in Fig.10.

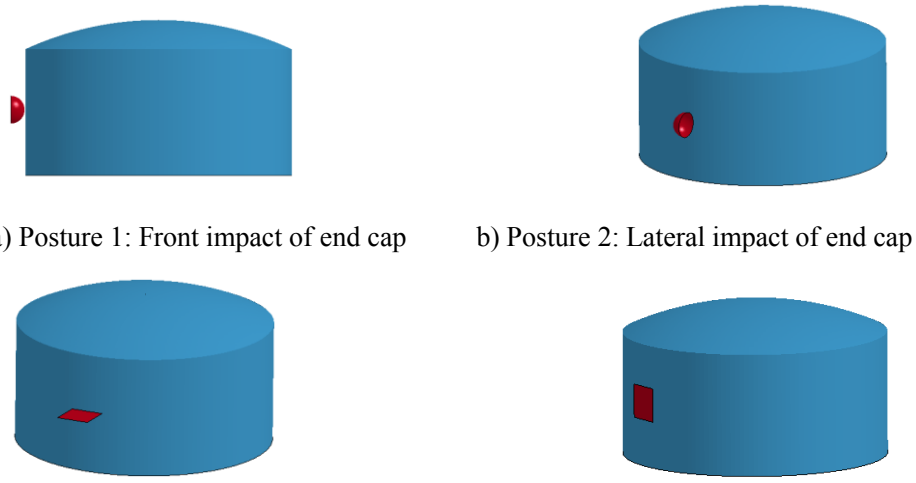

a) Posture 1: Front impact of end cap b) Posture 2: Lateral impact of end cap

c) Posture 3: Lateral impact of plate d) Posture 4: Front impact of plate

Fig.10 Impact postures

Fig.11 shows the displacement of impact center-time curve, the overall trend of 4 curves are roughly consistent. However, the displacement of the impact center for the case of Posture 1 is the maximum (about 1.85 m), while that for the case of Posture 4 is the minimum (about 1.33 m). The degree of deformation caused by the end cap is bigger than the plate. The degree of indentation caused by Posture 1 is greater than Posture 2, because the end cap was thin shell structure, lateral impact will cause serious deformation of the fragment itself. The fragment crimps seriously when the fragment impacts the tank with Posture 3. And 4 corners of the fragment slightly warp when the fragment impacts the tank with Posture 4. But the degree of indentation caused by Posture 3 is greater than Posture 4, the reason is that the effect of contact area between fragment and the tank is more significant, the smaller the contact area is, the more energy concentrates in the impact center.

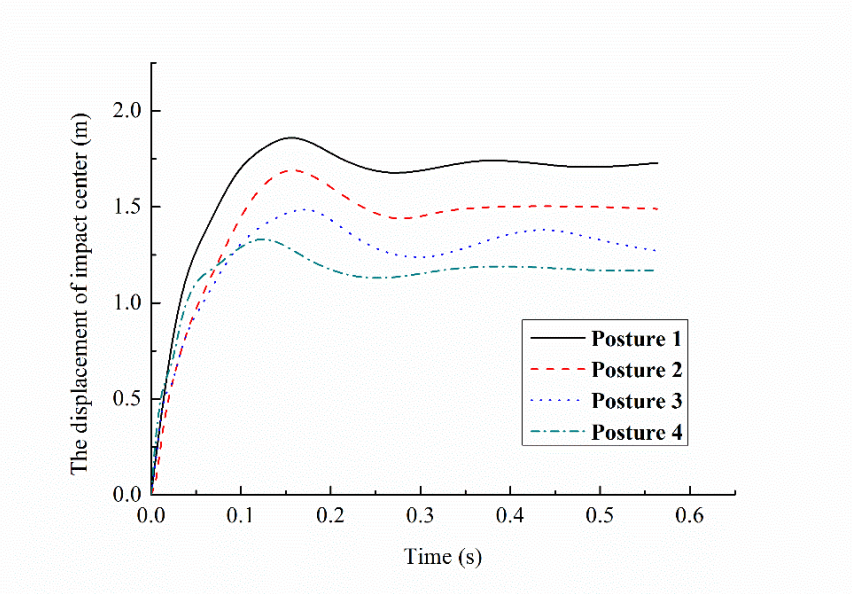

Fig.11 Displacement of impact center-time curve with four impact postures of fragments

Effect of impact velocity

The impact velocity of the fragment determines its kinetic energy and impulse, which would affect the force during impact and the final deformation of the tank. The 2297 kg end cap was used to impact the TK3 at velocity of 60 m/s, 65 m/s, 70 m/s, 75 m/s, 80 m/s, 85 m/s, and 90 m/s respectively. Table 8 shows the average acceleration and the displacement of impact center in each impact simulation. There are multiple collisions during the impact, therefore, the change of the fragment acceleration is complex and irregular. The average acceleration is defined by integrating the acceleration of the fragment with time, and divided by the impact time. It can reflect the impact force exerted in the tank during impact process.

Table 8 Average acceleration and the displacement of impact center

No.	Impact velocity (m/s)	Average acceleration (m/s^2)	The maximum displacement (m)	The residual displacement (m)	The recovery displacement (m)
1	60	416	1.85	1.70	0.15
2	65	440	1.98	1.83	0.15
3	70	456	2.10	1.95	0.15
4	75	464	2.22	2.07	0.15
5	80	563	--	--	--
6	85	605	--	--	--

7	90	753	--	--	--

As shown in Fig.12, the residual displacement of the impact center is linearly proportional to the impact velocity as the velocity ranges from 60 to 75 m/s. Table 8 indicates that all the recovery displacements of impact center are 0.15 m at velocity of 60~75 m/s, and the tank wall has entered the stage of plastic deformation. However, at velocity of 80~90 m/s, the tank wall is broken and no longer recovered, and the fragment penetrates the tank wall. Fig.13 shows the relationship between the average acceleration and the maximum displacement with impact velocity ranged from 60 to 75 m/s. The lager the maximum displacement is, the lager the average acceleration becomes, indicating that the average impact force exerted in the tank is larger. However, the increase rate of the average acceleration decreases gradually with the increase in the maximum displacement, which shows the plastic deformation appears in the tank, and the deformation resistance ability of the tank gradually decreases.

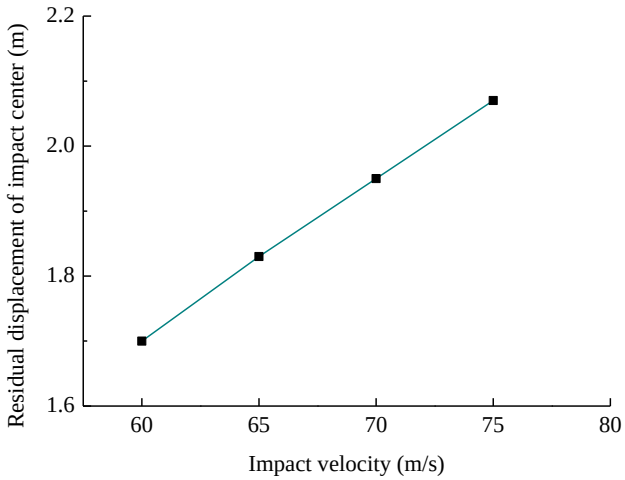

Fig.12 Relationship between residual displacement and impact velocity

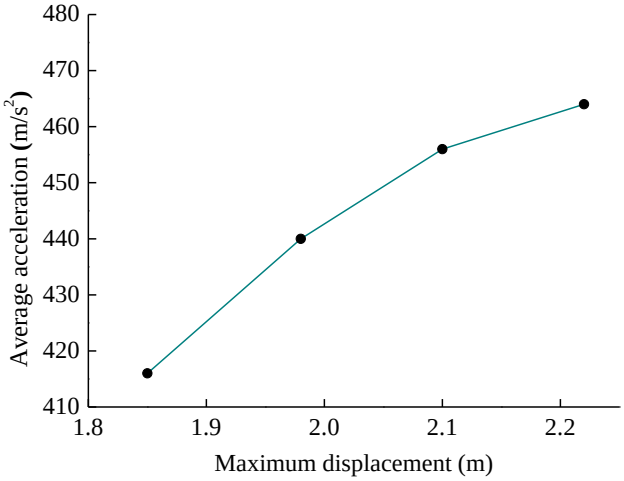

Fig.13 Relationship between average acceleration and maximum displacement of impact point

Effect of impact angle

Since the fragment may impact the tank at arbitrary angle and cause different effects on the tank, two kinds of angle, namely horizontal impact angle (HIA) and vertical impact angle (VIA), are considered. $\vec{v}_{\mathrm{i}}$ is decomposed into $\overrightarrow{v_{\mathrm{i}X}}$, $\overrightarrow{v_{\mathrm{i}Y}}$, $\overrightarrow{v_{\mathrm{i}Z}}$ as shown in Fig.14, O is arbitrary position on the tank wall, $\overrightarrow{v_{\mathrm{i}X}}$, $\overrightarrow{v_{\mathrm{i}Y}}$, $\overrightarrow{v_{\mathrm{i}Z}}$ can be calculated by Eq.(2)~Eq.(4).

$$v_{\mathrm{i}X} = v_{\mathrm{i}} \cdot \cos\theta \cdot \cos\omega \tag{2}$$

$$v_{\mathrm{i}Y} = -v_{\mathrm{i}} \cdot \sin\theta \tag{3}$$

$$v_{\mathrm{i}Z} = -v_{\mathrm{i}} \cdot \cos\theta \cdot \sin\omega \tag{4}$$

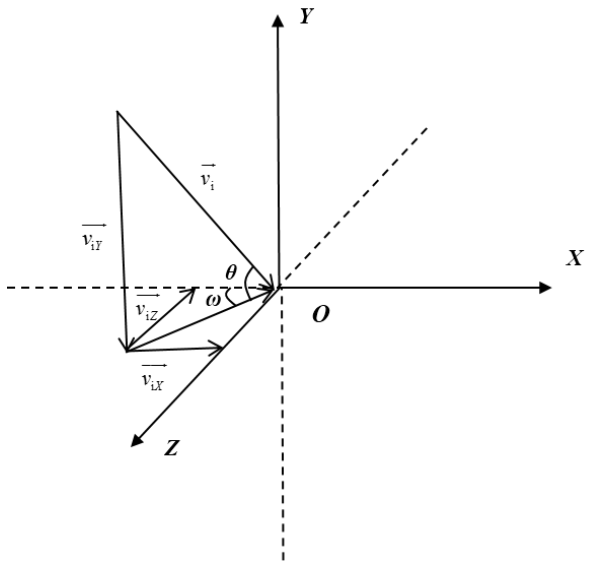

Fig.14 The decomposition of impact velocity

The 2297 kg end cap was used to impact the TK3 at 80 m/s, the tank deformation energy versus impact angle curve is shown in Fig.15. When HIA is in the range of 0°~15°, the curve slope is small, and HIA has little influence on the final tank deformation energy. When HIA is in the range of 15°~30°, HIA has significant influence on the tank deformation energy. And the larger the VIA is, the more serious the tank wall is penetrated, the higher deformation degree the tank wall performs. When HIA is in the range of 30°~35°, the impact mode of the fragment is changed from penetrating the tank wall to sliding along the tank wall, therefore, when HIA is 35°, fragment impacting on the tank with VIA of 0°causes the most serious deformation. The bigger the VIA is, the smaller the velocity component perpendicular to the tank wall is, the less deformation the tank performs. When HIA is in the range of 35°~60°, the fragment slides along the surface of the tank wall after contact, the tank deformation energy decreases with the increasing HIA and VIA. However, the effect of VIA on the tank deformation energy reduces significantly.

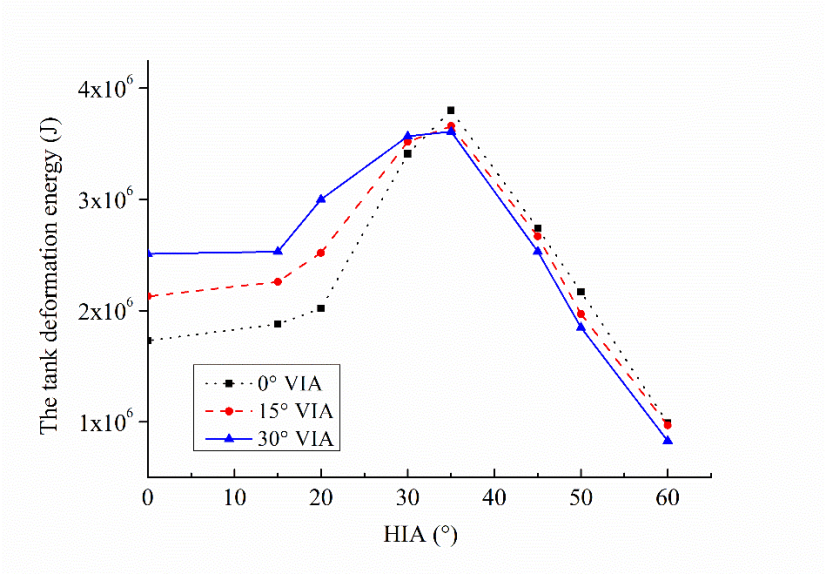

Fig.15 The tank deformation energy-impact angle curve

Conclusions

In this paper, dynamic response of vertical tanks impacted by blast fragments was investigated, the following conclusions could be obtained:

1) The process of the fragment impact on the tank included multiple collisions rather than only one collision. There were 3 collisions during the impact process of the end cap on the target tank at short time. The main deformation of the tank wall distributed near the impact center, the plastic strain was mainly appeared in the range from the impact center to the tank bottom.

2) The higher the impact location of the tank wall occurs, the more harmful will be to the tank wall. Compared with the plate-shaped fragment, the end cap-shaped fragment was more harmful to the target tank. When the impact velocity was in the range of 60~75 m/s, the residual displacement of the impact point increased linearly with the impact velocity, and all the recovery displacement of impact center were 0.15 m. The plastic deformation appeared in the tank, and the deformation resistance ability of the tank gradually decreased.

3) When HIA was in the range of 15°~30°, the HIA had significant influence on the tank deformation energy. When HIA was in the range of 30°~35°, the impact mode of the fragment was changed from penetrating the tank wall to sliding along the tank wall, the fragment impact on the tank with VIA of 0°caused the most serious deformation as HIA was 35°. When HIA was in the range of 35°~60°, the tank deformation energy was negatively linearly related to the HIA, and the effect of VIA on the tank deformation energy reduced significantly.

Acknowledgements

The research is supported by the National Natural Science Foundation of China (No. 21576102).

References

1. Arros J, Doumbalski N. Analysis of aircraft impact to concrete structures. Nuclear Engineering and Design. 2007;237:1241-9.
2. Atkinson G. Blast damage to storage tanks and steel clad buildings. Process Safety and Environmental Protection. 2011;89:382-90.
3. Wang Y, Zhou H. Numerical study of water tank under blast loading. Thin-Walled Structures. 2015;90:42-8.
4. Cui LF, Sun JG. Numerical simulation analysis of LNG outer tank mechanical properties under impact load. Journal of Natural Disasters. 2016;25:167-75.
5. Cozzani V, Antonioni G, Landucci G, Tugnoli A, Bonvicini S, Spadoni G. Quantitative assessment of domino and NaTech scenarios in complex industrial areas. Journal of Loss Prevention in the Process Industries. 2014;28:10-22.
6. Hemmatian B, Abdolhamidzadeh B, Darbra RM, Casal J. The significance of domino effect in chemical accidents. Journal of Loss Prevention in the Process Industries. 2014;29:30-8.
7. Mébarki A, Nguyen QB, Mercier F. Structural fragments and explosions in industrial facilities: Part II – Projectile trajectory and probability of impact. Journal of Loss Prevention in the Process Industries. 2009;22:417-25.
8. Nguyen QB, Mebarki A, Saada RA, Mercier F, Reimeringer M. Integrated probabilistic framework for domino effect and risk analysis. Advances in Engineering Software. 2009;40:892-901.
9. Chen G, Zhu JP, Wu J, Liu NA, Wang GD. Damage probability model of target storage tank impacted by explosion fragments. Journal of Disaster Prevention and Mitigation Engineering. 2012;32:216-22.
10. Pan XH, Xu J, Jiang JC, Wang ZR. Finite element simulation analysis on explosion debris impacting thin-wall cylindrical tanks. Journal of Nanjing University of Technology (Natural Science Edition). 2008;30:15-20.
11. Luo Y, Li XH, Wang JY. Numerical Simulation of Fragment Impact for the LPG Tank Failure. Industrial Safety and Environmental Protection. 2008;34:46-8.
12. GB 50128 Code for construction of vertical cylindrical steel welded storage tanks. 2014.
13. Gubinelli G, Cozzani V. Assessment of missile hazards: Evaluation of the fragment number and drag factors. Journal of Hazardous Materials. 2009;161:439-49.
14. Gubinelli G, Cozzani V. Assessment of missile hazards: Identification of reference fragmentation patterns. Journal of Hazardous Materials. 2009;163:1008-18.

15. NB/T 47001 Steel liquefied petroleum gas horizontal tank type and basic parameters. 2009.
16. Baum MR. Disruptive Failure of Pressure Vessels: Preliminary Design Guidelines for Fragment Velocity and the Extent of the Hazard Zone. Journal of Pressure Vessel Technology. 1988;110:168-76.
17. Safety CfCP. Guidelines for chemical process quantitative risk analysis. 2nd ed. New York: American Institute of Chemical Engineers; 2000.
18. Mebarki A, Bao Nguyen Q, Mercier F, Ami Saada R, Reimeringer M. Reliability analysis of metallic targets under metallic rods impact: Towards a simplified probabilistic approach. Journal of Loss Prevention in the Process Industries. 2008;21:518-27.
19. Jones N. Structural Impact. second ed ed. New York: Cambridge University Press; 2012.